Biochimica et Biophysica Acta 1827 (2013) 529–539

Contents lists available at SciVerse ScienceDirect

Biochimica et Biophysica Acta

journal homepage: www.elsevier.com/locate/bbabio

Two types of fucoxanthin-chlorophyll-binding proteins I tightly bound to the photosystem I core complex in marine centric diatoms

Yohei Ikeda [a,b,*], Atsushi Yamagishi [c], Masayuki Komura [c], Takehiro Suzuki [d], Naoshi Dohmae [d], Yutaka Shibata [c,1], Shigeru Itoh [c,2], Hiroyuki Koike [a,3], Kazuhiko Satoh [a]

[a] Graduate School of Life Science, University of Hyogo, Harima Science Garden City, Hyogo 678-1297, Japan
[b] Three-Dimensional Microscopy Research Team, RIKEN Harima Institute SPring-8 Center, 1-1-1 Kouto, Sayo, Hyogo 679-5148, Japan
[c] Division of Material Science (Physics), Graduate School of Science, Nagoya University, Furo-cho, Chikusa, Nagoya 464-8602, Japan
[d] Biomolecular Characterization Team, RIKEN Advanced Science Institute, Hirosawa 2-1, Wako, Saitama 351-0198, Japan

ARTICLE INFO

Article history:
Received 21 September 2012
Received in revised form 31 January 2013
Accepted 6 February 2013
Available online 14 February 2013

Keywords:
Photosystem I
Fucoxanthin-chlorophyll-binding protein I
Diatom
Chaetoceros gracilis
Thalassiosira pseudonana

ABSTRACT

Intact fucoxanthin (Fucox)-chlorophyll (Chl)-binding protein I-photosystem I supercomplexes (FCPI-PSIs) were prepared by a newly developed simple fast procedure from centric diatoms *Chaetoceros gracilis* and *Thalassiosira pseudonana* to study the mechanism of their efficient solar energy accumulation. FCPI-PSI purified from *C. gracilis* contained 252 Chl *a*, 23 Chl *c*, 56 Fucox, 34 diadinoxanthin + diatoxanthin, 1 violaxanthin, 21 ß-carotene, and 2 menaquinone-4 per P700. The complex showed a high electron transfer activity at 185,000 μmol mg Chl $a^{-1} \cdot h^{-1}$ to reduce methyl viologen from added cytochrome c_6. We identified 14 and 21 FCP proteins in FCPI-PSI of *C. gracilis* and *T. pseudonana*, respectively, determined by N-terminal and internal amino acid sequences and liquid chromatography–tandem mass spectrometry (LC–MS/MS) analyses. PsaO and a red lineage Chl*a*/*b*-binding-like protein (RedCAP), Thaps3:270215, were also identified. Severe detergent treatment of FCPI-PSI released FCPI-1 first, leaving the FCPI-2-PSI-core complex. FCPI-1 contained more Chl *c* and showed Chl *a* fluorescence at a shorter wavelength than FCPI-2, suggesting an excitation-energy transfer from FCPI-1 to FCPI-2 and then to the PSI core. Fluorescence emission spectra at 17 K in FCPI-2 varied depending on the excitation wavelength, suggesting two independent energy transfer routes. We formulated a model of FCPI-PSI based on the biochemical assay results.

1. Introduction

Diatoms occupy ecologically and phylogenetically unique positions and are the major primary producers in oceans contributing ~20% of the earth's annual net photosynthetic carbon fixation [1]. They use unique pigments, such as Chl *c* and Fucox, to efficiently capture light energy under limited light conditions. These pigments, as well as xanthophylls such as diadinoxanthin (Ddx) and diatoxanthin (Dtx), are associated with FCPs [2,3]. FCPs belong to the light-harvesting Chl-binding protein (LHC) superfamily [4], although LHCs in green algae and higher plants bind different pigments, Chl *b* and xanthophylls like lutein, violaxanthin (Vx), and zeaxanthin, on three transmembrane helices [5]. Whole genome analyses of two diatom species, *Thalassiosira pseudonana* and *Phaeodactylum tricornutum*, have suggested at least 30 [6] and 40 FCP candidates [7], respectively.

The roles and localizations of large numbers of FCPs of diatoms have not been clear. Phylogenic trees of the LHC superfamily suggested the ancestor of FCPs to be a red algal LHCI [8], which was classified as the Lhcr type (see Fig. S7). The standard clade (Lhcf type) FCPs are known to have different oligomeric states [9,10]. The LI818 Lhcx-type genes, Lhcx1/4/6, of *T. pseudonana* were reported to be upregulated in response to high light stress [11]. The distribution of multiple FCPs between photosystem (PS) I and II has not been clarified well because the hard silica shells around the cells of diatoms have interfered with the mild cell disruption required for the isolation of intact thylakoid membranes and complexes. Although some FCPs were isolated with PSI (hereafter designated as FCPI), the roles of multiple FCPIs associated with PSI have been poorly characterized (e.g., [12–15]). Recently, the stoichiometries of pigments bound to Lhcf-type FCPs and FCPII bound to the PSII [16] were reported.

Abbreviations: Chl, chlorophyll; PSI and PSII, photosystems I and II; LHC, light-harvesting chlorophyll-binding protein; FCPI, fucoxanthin-chlorophyll-binding protein I; LIL protein, light-harvesting-like protein; RedCAP, red lineage Chl*a*/*b*-binding-like protein; P700, primary electron donor chlorophyll dimer of Photosystem I; DDM, *n*-dodecyl-ß-D-maltoside; SDS–PAGE, sodium dodecyl sulfate–polyacrylamide gel electrophoresis; BN-PAGE, blue native polyacrylamide gel electrophoresis; SDG, sucrose density gradient; LC–MS/MS, liquid chromatography–tandem mass spectrometry; HPLC, high-performance liquid chromatography; Fucox, fucoxanthin; Ddx, diadinoxanthin; Dtx, diatoxanthin; Vx, violaxanthin; MK-4, menaquinone-4

* Corresponding author at: Three-Dimensional Microscopy Research Team, RIKEN Harima Institute SPring-8 Center, 1-1-1 Kouto, Sayo, Hyogo 679-5148, Japan. Tel.: +81 791581823.
E-mail address: yohei_ikeda@spring8.or.jp (Y. Ikeda).
[1] Current address: Department of Chemistry, Graduate School of Science, Tohoku University, Aoba, Sendai 980-8578, Japan.
[2] Current address: Center for Gene Research, Nagoya University, Furo-cho, Chikusa, Nagoya 464-8601, Japan.
[3] Current address: Department of Life Science, Faculty of Science and Engineering, University of Chuo, 1-13-27 Kasuga, Bunkyo, Tokyo 112-8551, Japan.

0005-2728/$ – see front matter © 2013 Elsevier B.V. All rights reserved.
http://dx.doi.org/10.1016/j.bbabio.2013.02.003

Trimeric and oligomeric free-FCPs were shown to bind pigments in the stoichiometries of Chl *a*:Chl *c*:Fucox = 7:2:6 and 8:2:5, respectively. On the other hand, the ratio in FCPII was 7:2:6. The putative binding sites of six Chl *a* (that correspond to a602, a603, a610, a612, a613, and a614 in LHCII) and one Chl *c* (that probably corresponds to b609 in LHCII) were conserved in Lhcf-type FCPs on the basis of the amino acid sequence homologies [10].

Recently, Neilson et al. reported one-, two-, three-, and four-helix light-harvesting-protein-like (LIL) sequences in photosynthetic eukaryotes, corresponding to high-light-induced proteins (HLIPs), stress-enhanced proteins (SEPs), early light-inducible proteins (ELIPs), and PsbS, respectively [17]. There were 2 one-helix and 1 two-helix LIL genes in *T. pseudonana* and 3 one-helix and 1 two-helix LIL genes in *P. tricornutum*. However, genes encoding proteins homologous to the PsbS (PsbS-like LIL) protein, which is known to be essential for the operation of the xanthophyll cycle in higher plants ([5,18]), have not been identified in the genomes of diatoms ([6,19]). Diatoms also have a xanthophyll cycle involving the conversion from Ddx to Dtx [20], which is similar to that in higher plants. The antenna system of diatoms, thus, seems to be composed of multiple proteins and might be regulated by molecular mechanisms somewhat different from those in other photosynthetic organisms, as seen in the tight coupling between the antenna proteins and PSI reaction center complex [21].

A higher-plant PSI complex seems to exist in a monomeric form made of 18 protein subunits (PsaA/B/C/D/E/F/G/H/I/J/K/L/N/O) including 4 LHCI (Lhca1-4) (see Fig. 7). Among them, PsaG/H/O/N are specific only for higher plants, and PsaO was not identified in the PSI structure revealed by X-ray crystallography [22] because PsaO is easily released [23]. LHCI subunits were bound to the PSI core at the side locations opposite to the binding sites of PsaH/L subunits. On the other hand, a cyanobacterial PSI complex, which forms trimers in the crystal without an antenna complex, is made of 12 protein subunits (PsaA/B/C/D/E/F/I/J/K/L/M/X) [24], in which PsaX is specific only for thermophilic cyanobacteria [25].

Bassi and Simpson [26] reported that LHCI could be separated by sucrose density gradient (SDG) centrifugation after mild treatment of the barley LHCI-PSI supercomplex with a 1% *n*-dodecyl-ß-D-maltoside (DDM). Bassi et al. [27] also reported the incomplete removal of LHCI from LHCI-PSI of a green alga, *Chlamydomonas reinhardtii*, by harsher treatment with 0.6% zwittergent 16 and 1% DDM, suggesting the tight binding of LHCI to the PSI core. We recently isolated an FCPI-PSI supercomplex (designated as FCPI-PSI, hereafter) from the intact thylakoid membranes of diatoms using a mild DDM treatment, which had a large molecular mass of ~1,050 kDa and contained more than 300 Chl *a* molecules with one PSI core [12]. Picosecond fluorescence analysis at low temperature indicated the efficient, and probably direct, excitation energy transfer from multiple FCPI to the PSI core and P700 [21].

In this study, we advanced the isolation procedure and adapted it to two species of diatoms. We isolated the homogeneous FCPI-PSI preparations, which had a ~900 kDa molecular mass and 250 Chl *a* with one PSI core. We further prepared an FCPI-PSI-core complex (designated as FCPI-PSI-core hereafter) by depleting two types of FCPI complexes (designated as FCPI-1 and FCPI-2) from FCPI-PSI (abbreviations were changed from those in a previous report [21] to accurately express the preparations). Biochemical and spectroscopic characterization of these preparations indicated that FCPI-PSI contains two types of FCPIs and that the FCP-PSI-core contains mainly FCPI-2. We have characterized multiple FCPI and FCPII constituents based on the amino acid sequences and discussed the arrangements and functions of FCPI-1 and FCPI-2 in PSI of diatoms.

2. Materials and methods

2.1. Diatom culture conditions

Two marine centric diatoms, *Chaetoceros gracilis* (UTEX LB2658) and *T. pseudonana* (CCMP 1335), were grown photoauotrophically for a week, as reported previously [12]. Diatom cells in the late logarithmic phase were collected by centrifugation (3000 ×*g*, 15 min) and washed twice in buffer A [50 mM 2-morpholinoethanesulfonic acid, monohydrate (MES)-NaOH (pH 6.0), 10 mM $MgCl_2$, 5 mM $CaCl_2$] supplemented with 25% glycerol (w/v). After re-suspending the pellet in buffer A supplemented with 1 M betaine, the collected cells were broken by freezing and stored at −80 °C until use.

2.2. Oxygen-evolving activity

Measurements of oxygen-evolving activity were performed as described in [12].

2.3. Purification of FCPI-PSI

Thylakoid membranes were isolated from *C. gracilis* and *T. pseudonana* as described by Ikeda et al. [12]. Intact thylakoid membranes equivalent to 1.0 mg Chl *a* L^{-1}were solubilized with 0.85–0.95% (w/v) DDM (Anatrace, Maumee, OH) for 10 min. The most effective concentration was determined by a preliminary solubilization test for each batch of culture. After removal of unsolubilized membranes by centrifugation (40,000 ×*g*, 10–15 min), the supernatant was diluted to decrease the DDM concentration to 0.1% with buffer A and then centrifuged at 40,000 ×*g* for 1 h (PSI-enriched fraction). The resulting pellet was resuspended in buffer B [5 mM MES-NaOH (pH 6.0) and 0.6% DDM]. The supernatant was loaded on a stepwise SDG with 6 mL solutions of 0.4 M, 0.6 M, and 0.8 M sucrose in buffer A supplemented with 0.05% DDM. After centrifugation (300,000 ×*g*, 1 h), the resulting pellet was resuspended in buffer B. After removal of the aggregated FCPI-PSI by centrifugation (9,000 ×*g*, 20 min), the supernatant was loaded on an anion exchange column (HiPrep 16/10 DEAE F, GE Healthcare Bio-Science, Buckinghamshire, UK). After being washed with 0.1 M NaCl for a short time, FCPI-PSI was eluted with a 0.1–0.5 M NaCl linear gradient in buffer A supplemented with 0.05% DDM at a flow rate of 2.0 mL min^{-1}. The elution was monitored at 280 nm using a SPD-6AV UV–VIS spectrophotometric detector (Shimadzu, Kyoto, Japan). The peak fractions at around 0.2 M NaCl were collected and concentrated using a filter membrane (NWCO; 100 kDa, Vivaspin, Sartorius Stedim Biotech, Aubagne, France).

2.4. Isolation of FCPI-PSI-core, FCPI-1, and FCPI-2 from C. gracilis

FCPI-PSI was suspended in 0.4 mg Chl *a* L^{-1} in buffer A supplemented with 0.05% DDM and solubilized with 15% (w/v) DDM for 30 min on ice. After effective solubilization by the detergent was confirmed by measuring the steady-state fluorescence emission at 77 K, the supernatant was diluted to decrease the DDM concentration to 0.5% with buffer A and then centrifuged through a filter membrane (NWCO; 100 kDa). Using the same procedure described above, a non-flow-through fraction (the crude FCPI-PSI-core fraction) and a flow-through fraction (crude FCPI) were diluted to decrease to 0.05% DDM with buffer A and centrifuged using a filter membrane (NWCO; 100 kDa and 30 kDa, respectively). By the second centrifugation, the crude FCPI-PSI-core fraction was separated into the FCPI-PSI-core and FCPI-2, and the crude FCPI was separated into FCPI-1 and non-colored flow-through fraction.

2.5. Polypeptide sequencing and LC–MS/MS analyses

SDS–PAGE, BN-PAGE, and N-terminal amino acid sequencing were performed as described in [28,12]. In-gel-digestion with *Achromobacter* protease I (API) [29] was carried out according to a previous report [30]. In the thermolitic digestions, excised Coomassie-stained gel bands were destained with 50% acetonitrile in 10 mM Tris–HCl (pH 8.0) and then dried *in vacuo*. The bands were incubated with 0.1 μg of thermolysin (Seikagaku Corporation, Tokyo, Japan) in 10 mM Tris–HCl (pH 8.0) at 37 °C for 12 h. The generated peptides were extracted from the gel

and separated on a column of Inertsil ODS-3 (3 μm, 1×100mm; GL Science Inc., Tokyo, Japan) with (API) or without (thermolysin) a precolumn of DEAE-5PW (1×20 mm; Tosoh, Tokyo, Japan) connected in tandem. Peptides were eluted at a flow rate of 20 μL/min using a linear gradient of 0–60% solvent B against solvent A, where solvents A and B were 0.09% (v/v) aqueous trifluoroacetic acid and 0.075% (v/v) trifluoroacetic acid in 80% (v/v) acetonitrile, respectively using a model 1100 series liquid chromatography system (Agilent Technologies, Waldbronn, Germany). Selected peptides were subjected to Edman degradation using a Procise HT or cLC protein-sequencing system (Applied Biosystems, Carlsbad, CA) to obtain the peptide sequences. LC–MS/MS using LCQ Deca XP plus (Thermo Fisher Scientific, Waltham, MA) was described previously [31].

The molecular weight was estimated by the trimeric PSI complexes and dimeric and monomeric PSII complexes from *Synechocystis* sp. PCC 6803 [32]. Lipids were extracted from FCPI samples before SDS–PAGE. SDS–PAGE results were quantified by densitometry by use of NIH Image 1.41 software using the density of carbonic anhydrase as the molecular standard in each gel.

2.6. Homology search and multiple sequence analyses

The homology search was conducted using NCBI BLAST (http://blast.ncbi.nlm.nih.gov/Blast.cgi), JGI *T. pseudonana* v3.0 (http://genome.jgi-psf.org/Thaps3/Thaps3.home.html), *P. tricornutum* v2.0 (http://genome.jgi-psf.org/Phatr2/Phatr2.home.html), and the diatom EST database (http://avesthagen.sznbowler.com/). Multiple sequence alignment was performed using ClustalX 2.0.12 software [33]. The bootstrap values were calculated in 1,000 iterations. The non-root neighbor-joining tree program was drawn using the NJplot program [34].

2.7. Analyses of pigments and quinones

The amounts of pigments and MK-4 were determined using HPLC according to [12].

2.8. Photochemical activities of P700

P700 was photooxidized by blue light obtained from a 100-W halogen lamp (Nikon, Tokyo, Japan) passed through a Corning 4–96 band-pass filter (Corning Inc., Corning, NY), and the P700 redox states were monitored at 701 nm with a UV–VIS spectrophotometer MPS 2000 (Shimadzu, Kyoto, Japan) at room temperature. The photodetector was protected with a Toshiba VR-68 filter (Toshiba, Tokyo, Japan). The reaction mixture contained 2 mM MV as an electron acceptor, 500 μM sodium ascorbate as an electron donor in buffer A supplemented with 1 M betaine, and thylakoid membranes corresponding to 30 μg Chl $a \cdot mL^{-1}$. In the measurement with FCPI-PSI, the reaction mixture contained 1 mM MV, 500 μM sodium ascorbate in buffer C [5 mM 2-[4-(2-hydroxyethyl)-1-piperazinly] ethanesulfonic acid (HEPES)-NaOH (pH 7.0) and 0.02% DDM], and FCPI-PSI equivalent to 20 μg Chl $a \cdot mL^{-1}$. The oxidation–reduction difference extinction coefficient of 70 $mM^{-1} \cdot cm^{-1}$ of P700 was used [35].

2.9. Light-induced redox change of P700

The flash-light-induced absorbance changes of FCPI-PSI were measured at 435 nm using a Photal RA401 stopped-flow spectrophotometer (Otsuka Electronics, Osaka, Japan) as reported previously [36].

2.10. Purification and photooxidation of cytochrome c_6

Cytochrome c_6 was prepared from *C. gracilis*, as reported in Koike and Katoh [37], with slight modifications. The photooxidation of cytochrome c_6 was measured at 553 nm, as for P700, as described above after an exchange of filters. The reaction mixture contained 1 mM MV as an electron acceptor, 20.5 μM reduced cytochrome c_6 in buffer D [50 mM Tris–HCl (pH 7.5) and 0.5 M NaCl], and an FCPI-PSI or thylakoid membranes equivalent to 0.4 μg and 10 μg Chl $a \cdot mL^{-1}$, respectively. The difference extinction coefficient of 2.1×10^4 $M^{-1} \cdot cm^{-1}$ at 553 nm was used.

2.11. Absorption and fluorescence spectroscopy

Absorption spectra at room temperature and at 77 K were measured using an MPS 2000 [12]. Steady-state fluorescence emission spectra at 77 K were measured using an H-20UV monochromator (Jobin Yvon, Cedex, France) with an MIC-7 controller (Horiba, Tokyo, Japan). Chromophores were excited by light supplied by a 100-W halogen lamp (Nikon, Tokyo, Japan) passed through a 4–96 band-pass filter (Corning, Corning, NY). The light excited Chl *a*, Chl *c*, and carotenoid. Absorption spectra at 4 K were measured according to Komura et al. [38].

2.12. Time-resolved fluorescence spectra and global analysis

Measurement of the time-resolved fluorescence spectra (TRFS) and global analysis of the fluorescence decay curve were performed with the excitation wavelengths at 430 or 460 nm at 17, 30, and 77 K, as described [21].

2.13. Fourth derivatives and Gaussian-deconvolution analysis

Fourth derivative spectra were calculated by the installed options of an MPS 2000 to search for the initial parameters for the simulation of absorption bands. The other parameters of each Gaussian-component band were estimated by a deconvolution program and adjusted to give common values for each absorption spectrum [38].

2.14. Electron microscopy

Electron microscopy analyses were carried out by negatively staining the samples with 2% (w/v) uranyl acetate using the transmission electron microscope 2010 (JEOL, Kyoto, Japan) set to calibrated magnifications of ×20,000, 50,000, and 100,000 at 100 kV.

3. Results

3.1. Isolation of FCPI-PSI from C. gracilis and T. pseudonana

We isolated almost intact thylakoid membranes from *C. gracilis* according to the method reported [12] and prepared FCPI-PSI by solubilizing the membranes with DDM. The DDM-solubilized membranes were, then, diluted with a DDM-free medium, and a PSI-enriched fraction was precipitated by the centrifugation, leaving the supernatant containing free FCPs. We assayed the polypeptide profiles of the membranes (lane 1 in Fig. 1) and PSI-enriched fraction (Fig. 1, lane 2). The free-FCP fraction gave four major bands, as shown in lane 1 in Fig. S1. The pellet was re-suspended in buffer B and loaded on a stepwise SDG to remove the 21 kDa free-FCP, which is indicated by an asterisk in Fig. 1. The resulting pellet was again suspended in buffer B and subjected to DEAE anion exchange chromatography to purify FCPI-PSI. The elution profiles of chromatography showed two main peaks of free-FCP and FCPI-PSI fractions at around 0.1 M and 0.2 M NaCl, respectively. The eluted FCPI-PSI fraction was collected and concentrated by passing through a size-exclusion filter. The purified FCPI-PSI contained 18–28-kDa "peripheral" FCPIs (Fig. 1, lane 3).

A similar isolation procedure was applied to *T. pseudonana* cells. Isolated thylakoid membranes of this organism showed a high electron transfer activity (~200 μmol O_2 mg^{-1} Chl *a* h^{-1}) in the presence of 0.5 mM 2,6-dichloro-*p*-benzoquinone as the electron acceptor at 30 °C. Purified FCPI-PSI contained multiple FCPIs, as seen with FCPI-PSI of *C. gracilis* (Fig. 1, lanes 5 and 6).

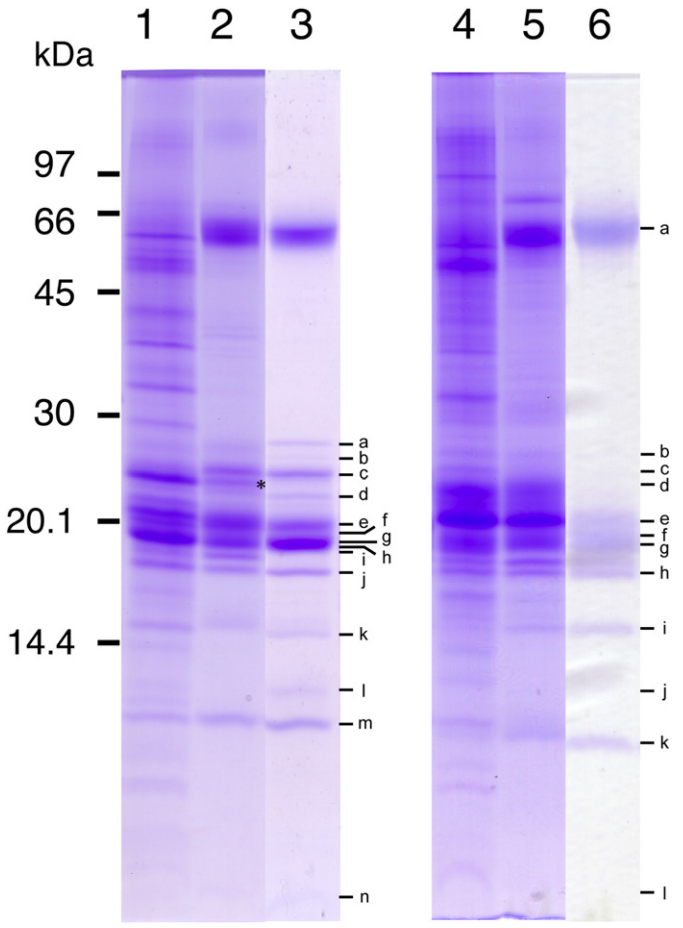

Fig. 1. Polypeptide profiles of *C. gracilis* and *T. pseudonana*. Lanes 1, thylakoid membranes; 2, PSI-enriched fraction; 3, FCPI-PSI from *C. gracilis*; 4, thylakoid membranes; 5, PSI-enriched fraction; 6, FCPI-PSI from *T. pseudonana*. All lanes were loaded with samples at 10 μg Chl *a*. The band labels a-n are the same as those in Table 2.

3.2. Photochemical activity of FCPI-PSI in C. gracilis

FCPI-PSI that was purified from *C. gracilis* was fully photoactive. Flash-light excitation induced rapid oxidation and subsequent slow dark re-reduction of $P700^+$ by electrons from photo-reduced intrinsic iron sulfur centers $(F_A/F_B)^-$ (Fig. S2, −MV) when monitored by the absorption change at 435 nm. In the presence of an artificial electron acceptor, methyl viologen (MV), the recovery kinetics showed a faster decay within 5 ms, demonstrating the rapid competitive oxidation of $(F_A/F_B)^-$ by MV (Fig. S2, +MV). The results showed that FCPI-PSI retains all the electron transport components from P700 to F_A/F_B in PSI.

To examine the intactness of the electron-donor side, the photooxidation of added cytochrome c_6 was monitored at 553 nm (Table 1). The oxidation rate of cytochrome c_6 was 185,000 μmol mg^{-1} Chl $a \cdot h^{-1}$ with saturating amounts of cytochrome c_6 and MV and much higher than that of 1,740 μmol mg^{-1} Chl $a \cdot h^{-1}$ of thylakoid membranes. The result indicates that the purified FCPI-PSI, which is depleted of PSII and a part of FCPs, still retains high activity for electron transfer.

3.3. Polypeptide compositions of FCPI-PSI preparations isolated from C. gracilis and T. pseudonana

The polypeptide compositions of FCPI-PSI isolated from the two diatom species are shown in Table 2 and Table S2. These data were obtained on the basis of the N-terminal and internal amino acid sequences and liquid chromatography–tandem mass spectrometry (LC–MS/MS) analyses. Gene models of *T. pseudonana* and *P. tricornutum* were also used for the identification of *C. gracilis* polypeptides. The PSI complex from *C. gracilis* contained 5 PSI core subunits: PsaC/D/F/J/O polypeptides. FCPI-PSI of *C. gracilis* contained 14 FCPs: Lhcr1/4/9/11/12/13, FCP2, Thaps3:6139/10219/270092/270215/270221/bd1160, and Tp17531. They reacted immunologically with specific antibodies against FCPs from the raphidophyte *Heterosigma akashiwo* except for Thaps3:6139 in our previous work [12]. The PSI complex from *T. pseudonana* contained 9 PSI core subunits: PsaA/B/C/D/E/F/J/L/O polypeptides. The FCPI-PSI from *T. pseudonana* contained 21 FCPs: Lhcr1/3/4/6/7/10/12/13/14, FCP2, Thaps3:6139/7916/10219/23808/270092/270215/bd1160, Tp17531, Lhcf1 or 2, Lhcf8 or 9, and Lhcf10 (Table 2). Eleven FCP proteins were common for the two FCPI-PSIs isolated from two diatom species. We also identified 1 and 3 FCP subunits in the free-FCP fraction of the SDG preparation from *C. gracilis* and *T. pseudonana*, respectively (Table S1).

3.4. Isolation of the FCPI-PSI-core, FCPI-1, and FCPI-2 from C. gracilis

Fig. 2 is a scheme of isolation of the FCPI-PSI-core, FCPI-1, and FCPI-2 from FCPI-PSI of *C. gracilis*. Sodium dodecyl sulfate–polyacrylamide gel electrophoresis (SDS–PAGE) analyses of these fractions were performed by loading them to give equivalent amounts of Chl *a* after extraction of lipids (Fig. 3). The polypeptide patterns of FCPI-1 and FCPI-2 showed bands at similar positions at 16–25 kDa with somewhat different densities (Fig. 3, lanes 2 and 3, and Fig. S3). A small amount of PsaA/B and a large amount of PsaO were also visible in FCPI-2 (Fig. 3, lane 3, and Fig. S3). The FCPI-PSI-core had lower amounts of FCPI polypeptides of around 20 kDa compared to those in the original FCPI-PSI with respect to PsaA/B bands (Fig. 3, lanes 1 and 4).

3.5. Molecular sizes of FCPI-PSI and the FCPI-PSI-core in C. gracilis

Blue native polyacrylamide gel electrophoresis (BN-PAGE) analyses in Fig. 4A suggest FCPI-PSI to be monomeric, as reported [12]. However, the molecular size at around 900 kDa in the present preparation (Fig. 4A, lane 1) is slightly smaller than that of 1,050 kDa of an FCPI-PSI preparation previously obtained by milder treatment [12]. The fractionated FCPI-PSI-core with a molecule size of 600–850 kDa seems to be also monomeric. The downsizings suggest the decreases in the amounts of FCPI subunits (Fig. 4A, lane 2). FCPI-1 and FCPI-2 could not be analyzed by BN-PAGE including 0.05% DDM because of their strong hydrophobicity.

We carried out electron microscopic analysis after negatively staining them (Fig. 4B). The particle sizes of FCPI-PSI were almost uniform, with a typical dimension of approximately 300×160 Å (Fig. 4B, left), while the sizes of the FCPI-PSI-core were smaller and non-uniform (Fig. 4B, right), in agreement with their different BN-PAGE patterns in Fig. 4A.

3.6. Analysis of absorption spectra of the isolated complexes from C. gracilis

Absorption spectra (Fig. 5) indicated higher contents of Chl *c* (~460 and ~635 nm) and carotenoids (~495 nm) in FCPI-PSI, FCPI-1, and FCPI-2 than in the FCPI-PSI-core, as seen from the spectra normalized

Table 1
Photo-oxidation rate of cytochrome c_6 purified from *C. gracilis*. Absorption changes were recorded at 553 nm. The difference extinction coefficient of cytochrome c_6 at 2.1×10^4 $M^{-1}cm^{-1}$ was used. Reaction mixtures contained 1 mM MV as an electron acceptor, purified cytochrome c_6 from *C. gracilis*, and the PSI-enriched fraction equivalent to 10-μg Chl *a* mL^{-1} in 50 mM Tris–HCl (pH 7.5) and 0.5 M NaCl (SD, $n=3$).

	Thylakoid membranes	FCPI-PSI fraction
Photo-oxidation rate of cytochrome c_6 μmol mg/Chl *a*/h	$(1.74\pm0.05)\times10^3$	$(1.85\pm0.04)\times10^5$

Table 2
Summary of subunit polypeptide compositions of FCPI-PSI of *C. gracilis* and *T. pseudonana* determined by N-terminal and internal amino acid sequencing and LC–MS/MS analyses. Exact peptide MS sequences are listed in Table S2. The table in parentheses shows the identity for *T. pseudonana* and *P. tricornutum*, respectively.

Polypeptide no.	N-terminal sequence	Internal sequence	Identified protein by N-terminal/internal sequence	Identified protein by LC MS/MS
Lane 3a	–	NMVPGLFDPFGF (83/—%)	Thaps3:6139	–
3b	xxAxDLELEAIKxNP (47/—%)	–	Thaps3:10219	–
3c	AMKDDLIAIAEKSNP (67/—%)	–	Thaps3:270092	–
	AMPERLxDSMVDKTE (60/73%)	DFGGFIQPPQxEEK (64/57%)	Lhcr11	
3d	AEINEAFGISIETGN (53/—%)	–	FCP2	–
3e	–	LYPTDPEKQQQM (33/67%)	Lhcr13	–
	–	xFDPLGxYP (56/78%)	Lhcr9	
3f	–	KLEQRMANYESG (58/58%)	PsaF	–
	–	EPGNLGFD (88/63%)	Lhcr13	
	–	GSPLPTIVFPPI (75/—%)	Thaps3:270221	
3 g	AIMKxxKLPFLPAPxNL (53/35%)	FGFDPL, VLTQGPFPY (87/93%)	Lhcr4	–
	–	KLEQRMANYESGxPPAL, NPAESEI (71/71%)	PsaF	
3 h	–	APANTAGYVGDVxFD (80/53%)	Lhcr1	–
	–	DENIIGITAPMGFFD (73/73%)	Tp17531	
	–	FSDYFPMDE (11/89%)	Lhcr12	
3i	VSVFDNYVxAKDFR (43/29%)	–	Thaps3:270215	–
	–	VQAMGKDERRPPGD (57/—%)	Thaps3:bd1160	
3j	–	IYRIFPSGEVQYLH, KYAITWT (100/100%)	PsaD	–
3 k	ANFIKPYNDDPFVG (100/100%)	–	PsaL [12]	–
3 l	–	SHTVKLYDTT (80/80%)	PsaC	–
3 m	VSRGSKVRILRKExY (73/67%)	–	PsaE [12]	–
	MAEDMTxEGEYPP (92/77%)	–	PsaO	
3n	MKNFQKYLSTAPVLL (87/93%)	–	PsaJ	–
lane 6a	–	–	–	PsaA
	–	–	–	PsaB
6b	–	–	–	Thaps3:10219
6c	–	–	–	Lhcr12
6d	–	–	–	FCP2
				Lhcf8 or Lhcf9
				Thaps3:270092
				Thaps3:6139
6e				Thaps3:23808
	AEMSKAMPFLINPANTDG	–	Lhcr1	Lhcr1
	EMSKxIPFLTVPEKLDGxM	–	Lhcr3	Lhcf1 or Lhcf2
	VDLDYGMKNxYVPATGG	–	Thaps3:268304	Lhcr6
				Thaps3:268304
6f				Lhcr4
	EMSKSIPFLTVPEKLD	–	Lhcr3	PsaF
	EIGGLTKxxExAAFTKRxNA	–	PsaF	Lhcr3
6 g				Tp17531
				Lhcr10
	xVAFNPEMA	–	Lhcr10	Lhcf10
	EIGxLPPTG	–	Lhcf10	Lhcr14
	AVKDxAE	–	Thaps3:270215	Lhcr13
				FCP_2
				Lhcr7
6 h	–	–	–	Thaps3:bd1160
6i	xLNLKTPFPxF	–	PsaD	–
6j	ANFIKPYNDDPFVGxLA	–	PsaL	PsaL
6 k	xxxTVKIYxT	–	PsaC	PsaC
6 l	IDRNSKVRILRKExY	–	PsaE	PsaE
	AEDMTxEGEYPP	–	PsaO	–
6 m	–	–	–	PsaJ

at Chl *a* peaks (670–680 nm). In the Q_y region, FCPI-PSI and the FCPI-PSI-core showed peaks at 677 nm with very similar bandwidths and pronounced shoulders at around 665 nm (Fig. 5, inset: black and magenta). The so-called red-Chl(s) bands in the PSI core were not identified at wavelengths over 700 nm. This was also the case for FCPI-PSI from *T. pseudonana* or *P. tricornutum*, suggesting the absence of typical red-Chls in the three diatoms (Fig. S4). FCPI-1 and FCPI-2 gave absorption peaks at 670 and 671 nm, respectively. FCPI-1 showed larger bandwidth than FCPI-2 in the Q_y region. The peak positions of two FCPI are shifted to the blue by 6–7 nm from those of FCPI-PSI and the FCPI-PSI-core (Fig. 5, inset: red and blue). FCPI-1 has higher contributions from Chl *c* and Ddx at 460 and 490 nm, respectively, than FCPI-2. Similar tendencies were detected at room temperature (Fig. S4, dashed line).

We performed Gaussian curve simulations using the spectra at 77 K (Fig. S5) starting from the initial peak positions deduced from the fourth derivative spectra. Table 3 summarizes the absorption peaks and bandwidths of the ten Gaussian component bands assumed for each complex. We fixed absorption peak of C628, which represents the Q_y band of Chl *c*. The simulations of four complexes indicated that they are composed of bands with very similar peak positions and bandwidths. All the peaks found in FCPI-PSI are also identified in other complexes, and no new peak seemed to appear by separation into the smaller complexes. FCPI-PSI, thus, seems to be made up as a mixture of component bands common with the FCPI-PSI-core, FCPI-1, and FCPI-2, suggesting a slight influence of the high-concentration detergent. The number of component bands for FCPI-1 was smaller than those of the other complexes. Short-wavelength Chl *a* bands were larger in FCPI-1 than in FCPI-2.

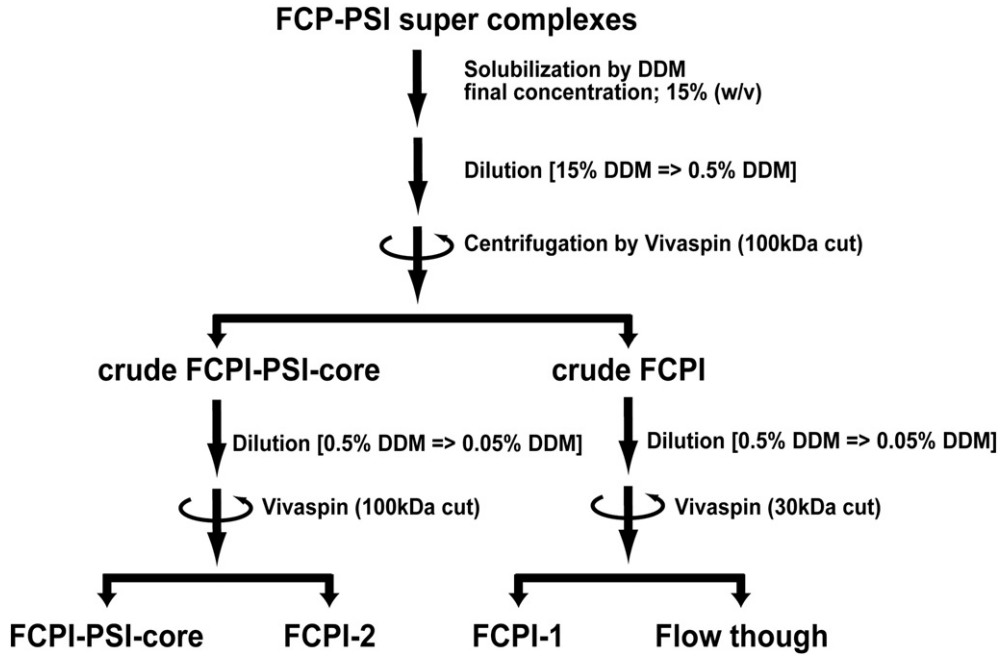

Fig. 2. Procedure for the isolation of each complex from the FCPI-PSI of *C. gracilis*. FCPI-PSI was solubilized with high-concentration DDM. The supernatant was diluted by a detergent-free buffer and centrifuged using a filter membrane. FCPI-PSI was separated into the FCPI-PSI-core, FCPI-1, and FCPI-2 and a non-colored flow-through fraction.

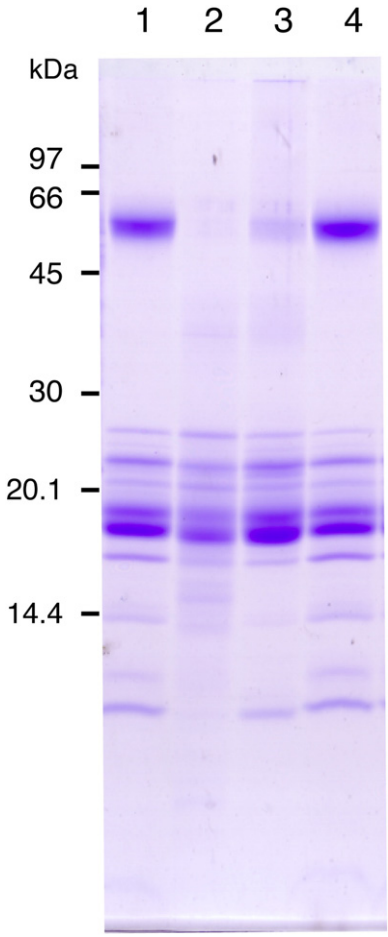

Fig. 3. Polypeptide profiles of FCPI-PSI (lane 1), FCPI-1 (lane 2), FCPI-2 (lane 3), and FCPI-PSI-core (lane 4) of *C. gracilis*. All lanes were loaded at the concentration of 10 μg Chl *a*.

3.7. Pigment compositions of the complexes isolated from C. gracilis

The pigment contents of purified complexes were analyzed by high-performance liquid chromatography (HPLC), as summarized in Table 4 on the basis of two menaquinone-4 (MK-4) molecules; one PSI unit contains two MK-4 as the secondary electron acceptor A_1 in PSI in the three diatoms [12], as do two phylloquinone molecules in PSI of other organisms. The amount of 252 Chl *a* molecules per two MK-4 agrees with the estimated antenna size of 255 (±9.7, $n=3$) Chl *a* per P700 by analysis of the photochemical activities, as described in Materials and methods section. In thylakoid membranes of *C. gracilis* grown in our laboratory, the ratio of Chl *a*/P700 was 1,346 (±58, $n=3$). The existence of 21 ß-carotene in FCPI-PSI and the FCPI-PSI-core also agrees well with the reported value of 22 ß-carotene in the cyanobacterial PSI complex [24]. This indicates that the PSI core of diatoms is very similar to that of other organisms. The other pigments, Chl *c*, Fucox, Ddx + Dtx, and Vx, as well as 100–150 Chl *a* on the FCPI-PSI-core and FCPI-PSI, are additional and seem to be bound to FCPI-1 and FCPI-2. The pigment compositions of the isolated FCPI-1 and FCPI-2 are also listed in Table 4 on the basis of 8 Chl *a*. The amount of Chl *a* in FCPI-1 was about four times that of FCPI-2 on the Chl *a* basis (data not shown). Therefore, if we add 40 Chl *a* on FCPI-1 and 10 Chl *a* on FCPI-2 to the pigments on the FCPI-PSI-core, which binds 205 Chl *a*, the sum of Chl *a* is close to that (252–255 Chl *a*) of the purified FCPI-PSI (Table 4). The above estimation was based on the assumption that FCPI-1 and FCPI-2 always bind fixed numbers of pigments per protein molecule.

The Chl *a*/*c* ratios of the purified FCPI-PSI, FCPI-PSI-core, FCPI-1, and FCPI-2 are calculated to be 10.8, 15.8, 4.1, and 8.1, respectively, based on Table 4. Chl *a*:Chl *c*:Fucox:Ddx + Dtx = 4.1:1.0:2.6:1.0 and 8.1:1.0:3.2:1.8 for FCPI-1 and FCPI-2, respectively. The above ratios may be approximated as 8:2:5:2 and 8:1:3:2, respectively. Thus, the stoichiometries of other pigments on FCPI-1 and FCPI-2 are also very different. It is, then, interesting that the contents of Chl *a* or Ddx + Dtx in the two complexes are almost identical. This suggests that FCPI-1 has one extra Chl *c* and two extra Fucox per 8 Chl *a* compared to FCPI-2.

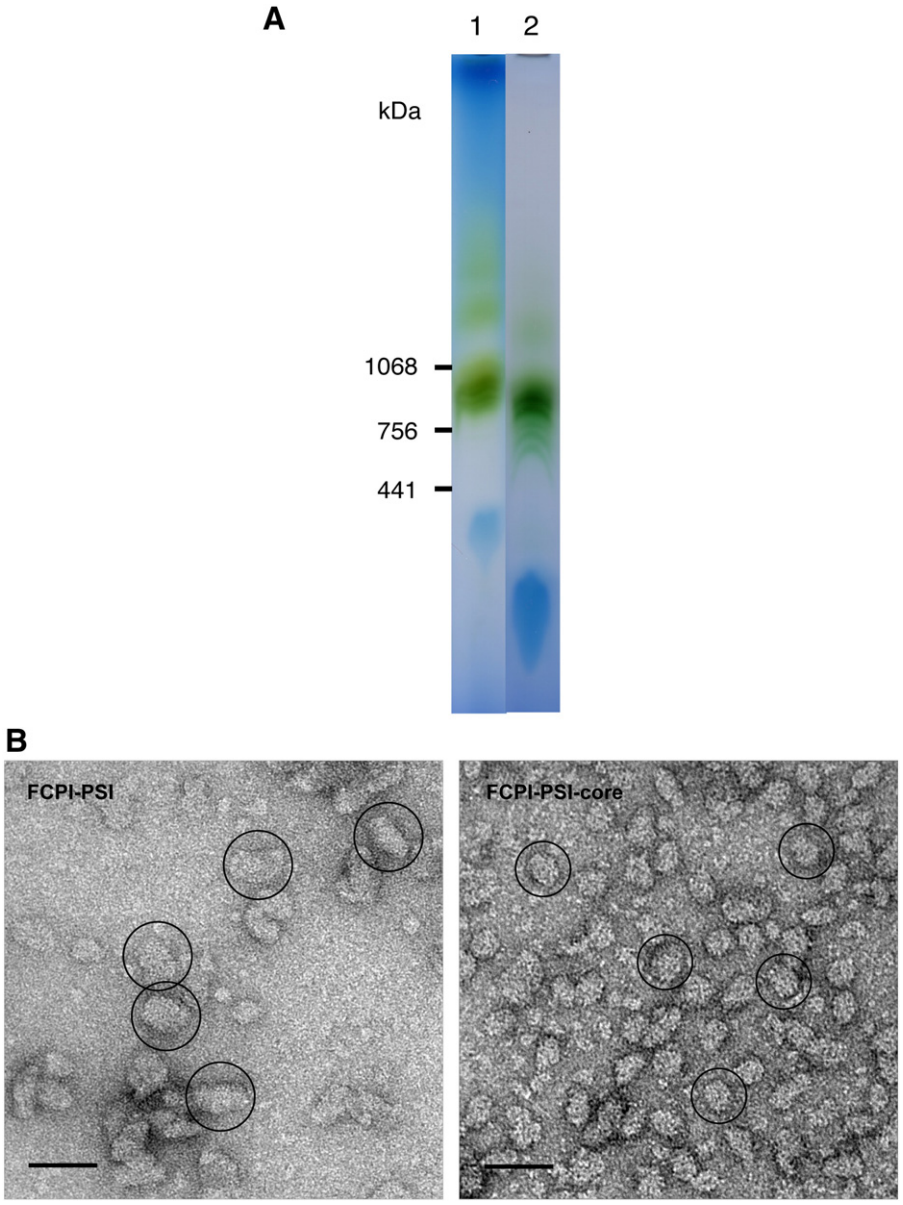

Fig. 4. A. Comparison of the BN-PAGE profiles of two complexes in *C. gracilis*. Lanes 1, FCPI-PSI; 2, FCPI-PSI-core. B. Electron microscopy images by negative staining. The calibrated magnification was ×50,000. The scale bar shows 40 nm. Left, FCPI-PSI; right, FCPI-PSI-core.

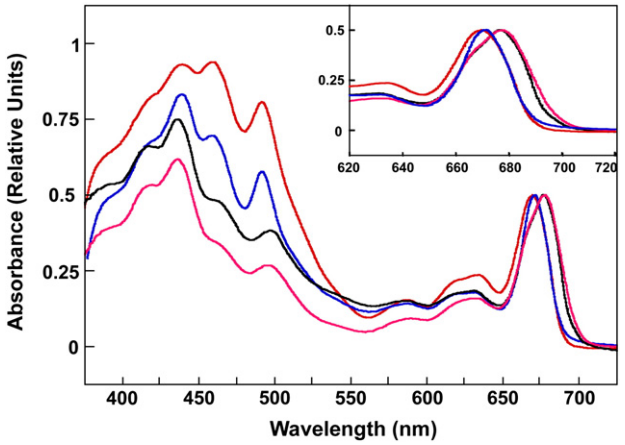

Fig. 5. Absorption spectrum at 77 K of each fraction from *C. gracilis*. Black, FCPI-PSI; magenta, FCPI-PSI-core; red, FCPI-1; blue, FCPI-2; inset, enlargement of the spectral range of 620–720 nm.

3.8. Fluorescence emission spectra of different complexes of C. gracilis

Fig. 6A shows the typical steady-state fluorescence emission spectrum of each fraction at 77 K excited with a 350–600-nm blue-green light. FCPI-PSI showed a fluorescence peak at 712 nm (Fig. 6A, black).

Table 3
Summary of absorption peaks and relative intensity per Chl *a* (%) estimated by the deconvolution analysis of absorption spectra at 77 K. Components with more than 7% contributions are shown. Bandwidth values were mainly 5–6 nm except for C628 (~40 nm) and C711 (~27 nm; ~1% relative intensity).

FCPI-PSI	627.7	659.8	666.7	674.5	680.4	686.8
	14.4	7.3	16.0	21.0	20.3	14.9
FCPI-PSI-core	629.5	658.4	666.4	673.9	680.0	687.5
	10.1	7.3	20.3	18.7	25.1	14.4
FCPI-1	627.8	657.8	665.3	672.7	680.0	
	19.4	10.0	21.9	28.0	16.1	
FCPI-2	624.6	659.2	665.9	672.7	680.2	
	16.4	8.6	16.8	36.2	14.1	

Upper/lower; wavelength peak (nm)/relative intensity per Chl *a* (%).

Table 4
Molar ratios of photosynthetic pigments in different complexes isolated from *C. gracilis* expressed on the basis of two MK-4 molecules (one PSI). These data show the standard deviation from five independent experiments.

Pigments	Chl *a*	Chl *c*	Fucox	Ddx + Dtx	Vx	ß-carotene	MK-4
FCPI-PSI	252[a] (±11.2)	23.4 (±1.67)	55.5 (±3.24)	34.4 (±2.32)	1.05 (±0.13)	20.5 (±0.78)	2.00
FCPI-PSI-core	205 (±11.6)	13.0 (±1.19)	29.8 (±3.40)	23.0 (±1.74)	0.80 (±0.14)	20.0 (±0.84)	2.00
FCPI-1	8.0	1.97 (±0.16)	5.20 (±0.35)	2.02 (±0.18)	0.04 (±0.01)	0.07 (±0.01)	-
FCPI-2	8.0	0.99 (±0.15)	3.01 (±0.49)	1.81 (±0.21)	0.05 (±0.01)	0.28 (±0.12)	-

[a] Chl *a*/P700 = 255 ± 9.7 (SD, *n* = 3).

Solubilization by DDM (Fig. 2) induced new fluorescence peaks at around 680 and 695 nm (Fig. 6A, magenta). The FCPI-PSI-core had a shoulder at around 670 nm, suggesting a small amount of loosely bound Chl *a* in the complex (Fig. 6A, green). FCPI-1 and FCPI-2 showed fluorescence peaks at 676–680 and 681–682 nm, respectively, from Chl *a* and at 639 nm from Chl *c* (Fig. 6A, red and blue). In FCPI-2, fluorescence peaks varied depending on the excitation wavelengths. Excitation at 430 and 460 nm gave emission peaks at 668 and 677 nm, respectively (Fig. 6B, lines *c* and *d*). This suggested the presence of at least two pigment pools, which seem to be unable to exchange excitation energy rapidly with each other. FCPI-1 showed a fluorescence peak at around 680 nm upon excitation at both 430 and 460 nm (Fig. 6B, lines *a* and *b*). These results are consistent with our previous observations [21]. Both samples had a small shoulder fluorescence band at around 700 nm, probably due to contamination of the PSI core.

We examined the energy transfer process inside FCPI-1 and FCPI-2, which showed different absorption and fluorescence spectra, by measurement of the ps fluorescence kinetics. Fig. S6 shows the time-resolved fluorescence spectra of FCPI-1 and FCPI-2 obtained using a streak-camera system at 17 K. The excitation energy transfer seemed to be effectively inside two FCPI, including FCPI-PSI and the FCPI-PSI-core [21], despite the strict detergent conditions.

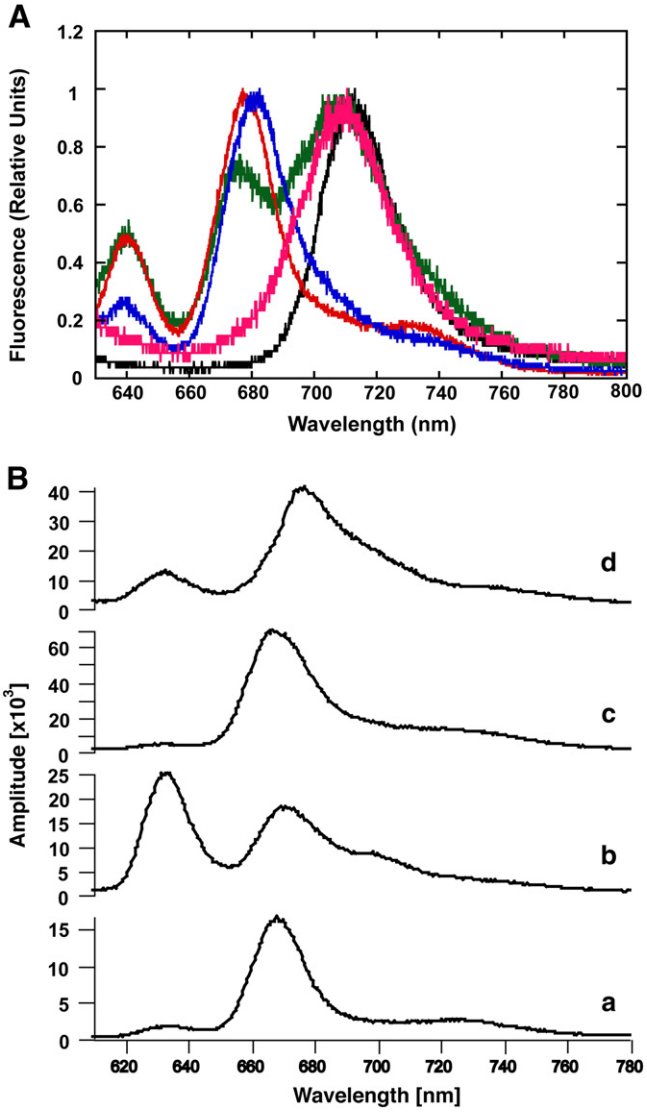

Fig. 6. A. 77 K fluorescence emission spectrum of each fraction from *C. gracilis*. Black, FCPI-PSI; magenta, solubilization of FCPI-PSI by DDM; red, FCPI-PSI-core; blue, FCPI-1; and line *e*, FCPI-2. B. 17 K steady-state fluorescence spectra of FCPI complexes. Lines a and b represent spectra of FCPI-1 excited at 430 and 460 nm, respectively, and lines c and d, FCPI-2 excited at 430 and 460 nm, respectively.

4. Discussion

4.1. Isolation of thylakoid membranes and purification of FCPI-PSI from two diatom species

We isolated FCPI-PSI from intact thylakoid membranes obtained with the freeze-thaw method from two species of diatoms, as previously reported [12]. The yield of FCPI-PSI was increased to ~3% of the starting thylakoid membranes on a Chl *a* basis in the present study. The yield is still low compared to the PSI purification procedures from cyanobacteria and higher plants. This comes primarily from the low contents of PSI in diatoms due to the abundance of FCPs and PSII. Pigment analysis by HPLC showed the pheophytin *a*:MK-4 ratio of thylakoid membranes to be 4–5:1, suggesting a high PSII/PSI ratio in both diatom species under our growth conditions. The purity as well as the efficiency of energy transfer from FCPI to P700 in the isolated FCPI-PSI of *C. gracilis* was improved from FCPI-PSI prepared previously, in which loosely bound FCPIs were still associated with FCPI-PSI [12]. SDS–PAGE analysis showed that the purified FCPI-PSI had less FCPI than the previously prepared FCPI-PSI [12]. The conclusion was supported by spectroscopic (Fig. 5) and pigment analyses (Table 4), which showed the smaller antenna size (255 ± 9.7 Chl *a*) and a smaller molecular size (Fig. 4A) of obtained the FCPI-PSI. If we assume the size and pigment content of the diatom PSI core to be the same as those of cyanobacterial PSI (356 kDa and 96 Chl *a*/22 β-carotene, respectively) and the average size of each FCPI subunit to be 19 kDa, we can calculate the number of FCPI subunits in one FCPI-PSI (two MK-4) prepared in this study to be ~18, which is a smaller value than ~23 recalculated on the basis of MK-4 in a previous study [12]. We, thus, assume FCPI subunits bound to diatom PSI to be heterogeneous. Grouneva et al. have also observed heterogeneous FCPI-PSI populations previously in 2D gel electrophoresis [15]. A similar situation seems to occur in *C. reinhardtii* LHCI because Stauber et al. [39] reported that PSI of *C. reinhardtii* contained only 7.5 LHCI subunits per PSI, although the PSI-LHCI complex contained 9 gene products [40].

Measurement of light-induced oxidation and dark reduction of P700 (Fig. S2) as well as the association with a peripheral PsaC subunit (Table 2) also confirmed the intactness of the FCPI-PSI prepared in this study. A very high photooxidation rate of reduced cytochrome c_6, which was purified from *C. gracilis*, was first confirmed in PSI. The rate was almost 100 times higher than that in the thylakoid membranes (Table 1). These results suggest that both the donor and acceptor sides of PSI in the purified FCPI-PSI are preserved in almost intact conditions.

4.2. Characterization of isolated FCPI-1 and FCPI-2 of C. gracilis

FCPI-1 and FCPI-2 showed similar behaviors on gel electrophoresis (Fig. S3), probably because of the limitation of densitometry analysis

on one-dimensional gel, which cannot distinguish co-migration bands, heterogeneous expressions, or nonstoichiometric amounts, as reported [39]. However, the pigment contents of two FCPIs differed significantly from each other. FCPI-1 and FCPI-2 showed different ratios of Chl *a*:Chl *c*:Fucox:Ddx + Dtx = 8:2:5:2 and 8:1:3:2, respectively. FCPI-PSI, therefore, contains at least two types of FCPI. This is also supported by the different fluorescence peaks and different peak ratios of Chl *c* to Chl *a* at 77 K (Fig. 6A). Gaussian deconvolution of the absorption spectra showed that a component Chl *a* peak at shorter wavelength is larger in FCPI-1 (Fig. S5). Single particle analysis revealed that LHCI was bound to the core complex on the same side as higher-plant LHCI, which makes double-layered belts, as seen in *C. reinhardtii* [41]. LHCI-680 and LHCI-705 have been reported to be clearly distinguishable by steady-state fluorescence spectra, although they were not clearly distinguished in SDS–PAGE [27]. The heterogeneous expression of lhca genes suggested the heterogeneities in the arrangement of LHCIs around PSI as well [39]. In *Arabidopsis thaliana*, a deleted mutant of the lhc4 gene had lhc5 at the lhc4 locus in purified PSI [42]. Arrangements of diatom FCPI, with high heterogeneity on the gene level, might be more complex than the arrangement of green algal or higher plant LHCI.

Fig. 6B shows the excitation-wavelength dependence of the fluorescence spectra of FCPI-2. The excitation of Chl *a* induced a 670 nm fluorescence peak of Chl *a*, and Chl *c* excitation induced a 680 nm fluorescence peak of Chl *a*, suggesting the existence of at least two pigment pools in FCPI-2, *i.e.*, Chl *a*, which gives 670 nm fluorescence seems, to be energetically coupled to neither Chl *c* nor Chl *a*, which gives fluorescence at 680 nm in the isolated FCPI-2. On the other hand, excitations of both Chl *a* and Chl *c* made FCPI-1 show almost the same fluorescence peaks. These results indicate the different excitation energy transfer processes inside FCPI-1 and FCPI-2.

4.3. Nature of FCPI tightly bound to the FCPI-PSI-core

First, we tried to deplete FCPI from FCPI-PSI to various extents, as described in earlier reports [26,27,43]. However, a treatment with a low concentration of DDM and/or Triton X-100 depleted only a small amount of FCPI or induced negligible loss of the fluorescence peak at 77 K of FCPI-PSI. Finally, we found that solubilization by 15% DDM separated FCPI-PSI into the FCPI-PSI-core and FCPIs without severe damage to their functions, as confirmed by the active excitation energy transfer observed by TRFS (Fig. S6). The requirement for the very high concentration of detergent suggests the very strong interaction between FCPI and the PSI core in diatoms as compared to barley [26] or *C. reinhardtii* [27], in which isolations of peripheral antenna from the PSI core complex typically require 0.6% zwittergent 16 and/or 1% DDM.

The cyanobacterial PSI complex is known to contain 96 Chl *a* molecules and 22 β-carotene [24]. On the other hand, the FCPI-PSI-core purified in this study still contained Chl *c* and higher numbers of Chl *a* together with 21 β-carotene and 2 MK-4 (one PSI core). Subtraction of 96 Chl *a*, which is expected to reside on the PSI core, from the pigment composition of the FCPI-PSI-core results in the residual pigment composition of Chl *a* Chl *c*:Fucox:Ddx + Dtx = 109:13:30:23. The ratio is approximately 8:1:2:2, suggesting that the FCPI-PSI-core contained FCPI with a pigment composition very similar to that of FCPI-2. The fluorescence measurement also showed that loosely bound FCPI of the FCPI-PSI-core depended on the excitation wavelength, as seen in the isolated FCPI-2 [21]. These results indicate that the FCPI remaining on the FCPI-PSI-core is FCPI-2.

4.4. Polypeptide compositions of FCPI-PSI of C. gracilis and T. pseudonana

On the PSI core of diatoms, whole genome sequence analyses have suggested the presence of ten polypeptide subunits (PsaA/B/C/D/E/F/I/J/L/M). We identified the PsaC/D/F/J/O and PsaA/B/C/D/E/F/J/L/O subunits, respectively, in FCPI-PSI of *C. gracilis* and *T. pseudonana* in this study in addition to previously identified PsaL and E subunits of *C. gracilis* PSI [12]. The PsaO subunits in two diatoms were first identified in this study. The mature PsaO subunit had 2 transmembrane helices with a 7 kDa molecular mass, like the PsaE polypeptide [44,12]. The identity between the amino acid sequences of the PsaOs of *T. pseudonana* and *P. tricornutum*, including the signaling sequences, was only 55%. To date, PsaO proteins have been discovered in two red algae, *Galdieria sulphuraria* [45] and *Cyanidioschyzon merolae* [CMP086C]; one cryptophyta, *Guillardia theta*; one brown algae, *Ectocarpus siliculosus* [Esi_0121_0043]; three diatoms, *C. gracilis* and *T. pseudonana* as well as *P. tricornutum* [Phatr2:42506]; and a number of other green algae and higher plants. In *A. thaliana* PSI complexes, PsaO is suggested to be located close to PsaL on the PsaH/L/I side of the PSI core and to keep the balance of excitation energy distribution between the two photosystems [46]. The role of PsaO in diatom PSI remains to be studied. Thaps3:268304 was also found [15].

So far, 12 Lhcr proteins have been identified: Lhcr1/2/3/4/7/10/11/12/13/14/23808/bd1160 [13–15]. Among these, Lhcr2 and Lhcr12 were identified only for *P. tricornutum*, while Lhcr7 and bd1160 were identified only for *T. pseudonana* [14,15]. In this study, 9 Lhcr proteins were first identified: Lhcr6/9, FCP2, and Thaps3:6139/7916/10219/270092/270215/270221. We also identified 11 proteins as common members in PSI of the two species (Fig. S7, red); thus, we identified at least 24 different FCPs in this study, as listed in Table 2.

4.5. Phylogeny of the FCP superfamily in T. pseudonana

Fig. S7 shows a phylogenic tree of the FCP superfamily in *T. pseudonana* that is formulated together with the results in the present study. We used the JGI *T. pseudonana* v3.0 website to obtain the amino acid sequences of FCPs with protein IDs and user annotations (Table S3). Based on multiple alignment analyses, we constructed a non-rooted neighbor-joining tree. There were four subclades: Lhcr, Lhcf, and Lhcx types, as well as a newly identified member of LIL type. The Lhcr subclade had many FCP members and the widest diversity. All the identified FCP subunits in FCPI-PSI were categorized as the Lhcr type (see Fig. S7) except for four Lhcf polypeptides, Tp17531, Lhcf1 or 2, Lhcf8 or 9, and Lhcf10 in *T. pseudonana*.

The phylogenic tree suggests that Thaps3:270215 was categorized as the LIL type. Thaps3:270215 is assumed to be ELIP on the JGI website according to the annotation by Gruber. On the contrary, Green did not assign it to ELIP because of the absence of an ELIP clade on JGI. Recently, Engelken et al. [47] reported that Thaps3:270215 was a member of the red lineage Chl*a*/*b*-binding-like protein (RedCAP). The presence of RedCAP was confirmed in two species of diatoms, *T. pseudonana* and *P. tricornutum* and one red alga species, *G. sulphuraria* [47]. Its putative homologs were also found in a red alga, *Griffithsia japonica*, a pelagophyte alga, *Aureococcus anophagefferens* [AURANDRAFT_25646], *Thalassiosira oceanica* [THAOC_01290], *E. siliculosus* [Esi_0256_0036], and *G. theta* in our blast search. The putative binding sites of three Chl *a*, which correspond to a602, a610, and a612 in LHCII, were conserved in RedCAP proteins in our multiple sequence analyses. Our phylogenic tree suggests Thaps3:270215 protein as a member of LIL because this branch was supported by a relatively strong bootstrap value (862/1000). We conclude, therefore, that Thaps3:270215 is a novel three-helix LIL protein, which was not described previously [17], and is first reported as the RedCAP protein, which is only found in the red lineage, bound to the PSI complex of two species of diatoms.

4.6. A model structure of FCPI-PSI in centric diatoms

Fig. 7A shows a schematic structural model of FCPI-PSI. We located FCPI-2 closer to the PSI core than FCPI-1. The FCPI subunits remaining in the FCPI-PSI-core must be of the FCPI-2 type because the calculated pigment ratio for FCPI is close to that for FCPI-2. The tighter binding of

FCPI-2 to the core complex suggested by the DDM-treatment experiments supports the above assignment. On the other hand, the pigment composition of FCPI-1 was very similar to that of oligomeric free-FCPs [10]. One molecule of Vx, a typical xanthophyll-cycle pigment in other organisms, is also assumed to be located in the FCPI-PSI-core. It might exist close to the PSI core. No difference was detected in the amino acid sequences of the two FCPI in the analysis of the multiple sequence alignment. Six Chl *a* (a602, a603, a604, a610, a612, and a613) and one Chl *c* (b609) putative binding sites were conserved in Lhcr-type FCPs of *T. pseudonana* in our sequence analysis. The conservation of the Chl *a*, a614, depends on the amino acid lengths. Helix2, which has most of the Chl *c* putative binding sites (b605, b606, b607, and b608, except for b601), shows low sequence similarity. Thus, presumably the variety in the amino acid sequence might be the origin of the differences in FCPI, such as FCPI-1 and FCPI-2.

PSI cores are known to be surrounded by double-layered LHCIs on the PsaF side in green algae PSI (Fig. 7B, c) [41] and by single-layered LHCIs in the PSI of higher plants (Fig. 7B, b) [22]. Thus, the PsaO protein in higher plants and green algae might be easily released during the preparation of PSI complexes, as assumed by Ozawa et al. [23] because of the absence of the capping LHCs [22]. PsaO in a diatom, however, might not be exposed to the outer aqueous phase until the removal of FCPI by the first treatment of FCPI-PSI with a high concentration of DDM. FCPI might bind to the PSI core on both the PsaL and PsaF sides as well (Fig. 7B, d).

The protein–protein interaction between the PSI core and FCPI-2 seems to be very tight, in agreement with the conclusion by Yamagishi et al. [21], who assumed the direct ultra-rapid excitation energy transfer from FCPI-1 to the PSI core. We drew FCPI-1 and FCPI-2 as small ovals in Fig. 7B, although their localizations are unknown.

5. Conclusions

We have purified intact FCPI-PSI from two diatom species. FCPI-PSI contains about 18 FCPI. FCPI-1 and FCPI-2 differ markedly from each other in the pigment compositions and spectroscopic properties, although two FCPIs were not clearly distinguished in SDS–PAGE. About 12 FCPI-2 in the FCPI-PSI-core bound to the PSI core very tightly. This is consistent with the direct transfer excitation energy from FCPI-2 to PSI [21].

Acknowledgments

We thank Dr. Teruhisa Hirai for helpful discussions in the EM experiment. This work was supported by grants from the Global Center of Excellence Program (GCOE) from the Ministry of Education, Culture, Sports, Science and Technology, Japan (K.S.).

Appendix A. Supplementary data

Supplementary data to this article can be found online at http://dx.doi.org/10.1016/j.bbabio.2013.02.003.

References

[1] C.B. Field, M.J. Behrenfeld, J.T. Randerson, P. Falkowski, Primary production of the biosphere: integrating terrestrial and oceanic components, Science 281 (1998) 237–240.
[2] G. Guglielmi, J. Lavaud, B. Rousseau, A.L. Etienne, J. Houmard, A.V. Ruban, The light-harvesting antenna of the diatom *Phaeodactylum tricornutum*. Evidence for a diadinoxanthin-binding subcomplex, FEBS J. 272 (2005) 4339–4348.
[3] A. Beer, K. Gundermann, J. Beckmann, C. Büchel, Subunit composition and pigmentation of fucoxanthin-chlorophyll proteins in diatoms: evidence for a subunit involved in diadinoxanthin and diatoxanthin binding, Biochemistry 45 (2006) 13046–13053.
[4] D. Durnford, R. Aebersold, B. Green, The fucoxanthin-chlorophyll proteins from a chromophyte alga are part of a large multigene family: structural and evolutionary relationships to other light harvesting antennae, Mol. Genet. Genomics 253 (1996) 377–386.
[5] R.C. Bugos, H.Y. Yamamoto, Molecular cloning of violaxanthin de-epoxidase from romaine lettuce and expression in *Escherichia coli*, Proc. Natl. Acad. Sci. U. S. A. 93 (1996) 6320–6325.
[6] E.V. Armbrust, J.A. Berges, C. Bowler, B.R. Green, D. Martinez, N.H. Putnam, S. Zhou, A.E. Allen, K.E. Apt, M. Bechner, M.A. Brzezinski, B.K. Chaal, A. Chiovitti, A.K. Davis, M.S. Demarest, J.C. Detter, T. Glavina, D. Goodstein, M.Z. Hadi, U. Hellsten, M. Hildebrand, B.D. Jenkins, J. Jurka, V.V. Kapitonov, N. Kroger, W.W. Lau, T.W. Lane, F.W. Larimer, J.C. Lippmeier, S. Lucas, M. Medina, A. Montsant, M. Obornik, M.S. Parker, B. Palenik, G.J. Pazour, P.M. Richardson, T.A. Rynearson, M.A. Saito, D.C. Schwartz, K. Thamatrakoln, K. Valentin, A. Vardi, F.P. Wilkerson,

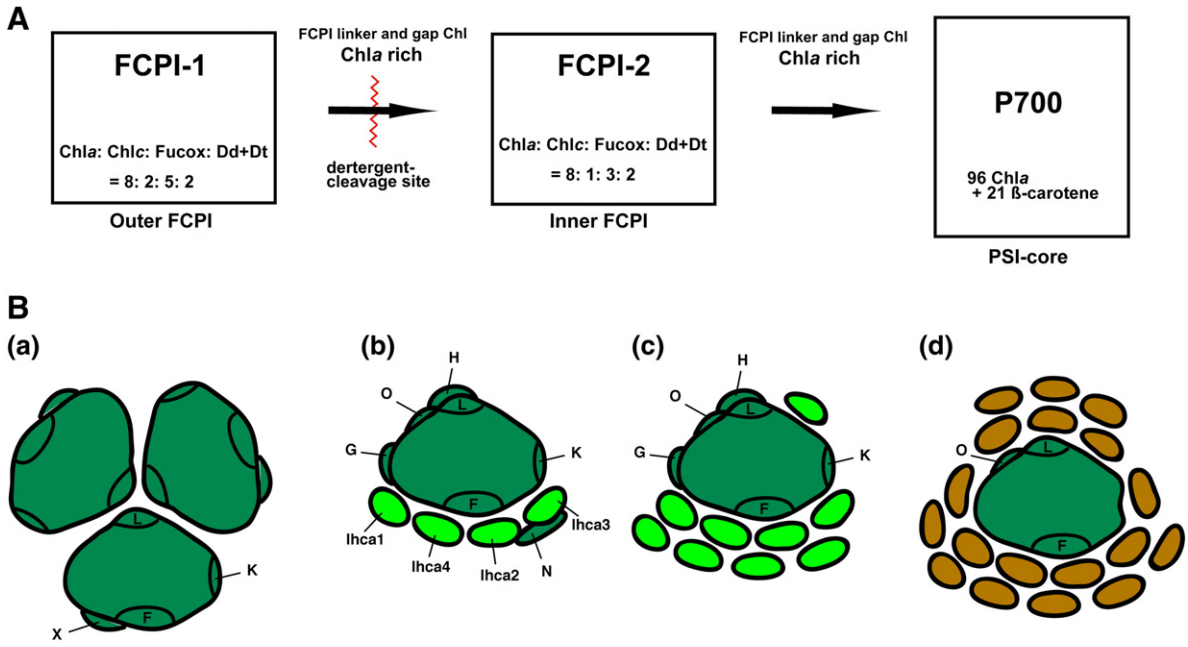

Fig. 7. A. A model of the pigment compositions in FCPI-PSI. The pigment stoichiometries of FCPI-1 and FCPI-2 are Chl *a*:Chlc:Fucox:Ddx + Dtx = 8:2:5:2 and 8:1:3:2, respectively. The arrows indicate the excitation energy flow. The zigzag red line indicates the detergent-cleavage sites. B. Models of the subunit compositions in PSI super complexes from various organisms. a, Cyanobacterial PSI. Trimeric PSI is shown in dark-green [24]; b, higher-plant PSI. Monomeric PSI and 4 LHCI are shown in dark-green and light-green circles, respectively [22]; c, green algae PSI. Monomeric PSI and 9 LHCI are shown in dark-green and light-green circles, respectively [39]; d, diatom FCPI-PSI. Monomeric PSI and 6 FCPI-1 and 12 FCPI-2, surrounding the core complex, are shown in dark-green and brown circles, respectively.

D.S. Rokhsar, The genome of the diatom *Thalassiosira pseudonana*: ecology, evolution, and metabolism, Science 306 (2004) 79–86.
[7] M. Nymark, K.C. Valle, T. Brembu, K. Hancke, P. Winge, K. Andresen, G. Johnsen, A.M. Bones, An integrated analysis of molecular acclimation to high light in the marine diatom *Phaeodactylum tricornutum*, PLoS One 4 (2009) e7743.
[8] D. Durnford, J. Deane, S. Tan, G. McFadden, E. Gantt, B. Green, A phylogenetic assessment of the eukaryotic light-harvesting antenna proteins, with implications for plastid evolution, J. Mol. Evol. 48 (1999) 59–768.
[9] C. Büchel, Fucoxanthin-chlorophyll proteins in diatoms: 18 and 19 kDa subunits assemble into different oligomeric states, Biochemistry 42 (2003) 13027–13034.
[10] L. Premvardhan, B. Robert, A. Beer, C. Buchel, Pigment organization in fucoxanthin chlorophyll *a*/*c*(2) proteins (FCP) based on resonance Raman spectroscopy and sequence analysis, Biochim. Biophys. Acta 1797 (2010) 1647–1656.
[11] S.H. Zhu, B.R. Green, Photoprotection in the diatom *Thalassiosira pseudonana*: Role of LI818-like proteins in response to high light stress, Biochim. Biophys. Acta 1797 (2010) 1449–1457.
[12] Y. Ikeda, M. Komura, M. Watanabe, C. Minami, H. Koike, S. Itoh, Y. Kashino, K. Satoh, Photosystem I complexes associated with fucoxanthin-chlorophyll-binding proteins from a marine centric diatom, *Chaetoceros gracilis*, Biochim. Biophys. Acta 1777 (2008) 351–361.
[13] T. Veith, J. Brauns, W. Weisheit, M. Mittag, C. Buchel, Identification of a specific fucoxanthin-chlorophyll protein in the light harvesting complex of photosystem I in the diatom *Cyclotella meneghiniana*, Biochim. Biophys. Acta 1787 (2009) 905–912.
[14] B. Lepetit, D. Volke, M. Gilbert, C. Wilhelm, R. Goss, Evidence for the existence of one antenna-associated, lipid-dissolved and two protein-bound pools of diadinoxanthin cycle pigments in diatoms, Plant Physiol. 154 (2010) 1905–1920.
[15] I. Grouneva, A. Rokka, E.M. Aro, The thylakoid membrane proteome of two marine diatoms outlines both diatom-specific and species-specific features of the photosynthetic machinery, J. Proteome Res. 10 (2011) 5338–5353.
[16] R. Nagao, T. Tomo, E. Noguchi, S. Nakajima, T. Suzuki, A. Okumur, Y. Kashino, M. Mimuro, M. Ikeuchi, I. Enami, Purification and characterization of a stable oxygen-evolving Photosystem II complex from a marine centric diatom, *Chaetoceros gracilis*, Biochim. Biophys. Acta 1797 (2010) 160–166.
[17] J.A. Neilson, D.G. Durnford, Evolutionary distribution of light-harvesting complex-like proteins in photosynthetic eukaryotes, Genome 53 (2010) 68–78.
[18] X.P. Li, O. Bjorkman, C. Shih, A.R. Grossman, M. Rosenquist, S. Jansson, K.K. Niyogi, A pigment-binding protein essential for regulation of photosynthetic light harvesting, Nature 403 (2000) 391–395.
[19] C. Bowler, A.E. Allen, J.H. Badger, J. Grimwood, K. Jabbari, A. Kuo, U. Maheswari, C. Martens, F. Maumus, R.P. Otillar, E. Rayko, A. Salamov, K. Vandepoele, B. Beszteri, A. Gruber, M. Heijde, M. Katinka, T. Mock, K. Valentin, F. Verret, J.A. Berges, C. Brownlee, J.P. Cadoret, A. Chiovitti, C.J. Choi, S. Coesel, A. De Martino, J.C. Detter, C. Durkin, A. Falciatore, J. Fournet, M. Haruta, M.J. Huysman, B.D. Jenkins, K. Jiroutova, R.E. Jorgensen, Y. Joubert, A. Kaplan, N. Kroger, P.G. Kroth, J. La Roche, E. Lindquist, M. Lommer, V. Martin-Jezequel, P.J. Lopez, S. Lucas, M. Mangogna, K. McGinnis, L.K. Medlin, A. Montsant, M.P. Oudot-Le Secq, C. Napoli, M. Obornik, M.S. Parker, J.L. Petit, B.M. Porcel, N. Poulsen, M. Robison, L. Rychlewski, T.A. Rynearson, J. Schmutz, H. Shapiro, M. Siaut, M. Stanley, M.R. Sussman, A.R. Taylor, A. Vardi, P. von Dassow, W. Vyverman, A. Willis, L.S. Wyrwicz, D.S. Rokhsar, J. Weissenbach, E.V. Armbrust, B.R. Green, Y. Van de Peer, I.V. Grigoriev, The Phaeodactylum genome reveals the evolutionary history of diatom genomes, Nature 456 (2008) 239–244.
[20] R. Goss, T. Jakob, Regulation and function of xanthophyll cycle-dependent photoprotection in algae, Photosynth. Res. 106 (2010) 103–122.
[21] A. Yamagishi, Y. Ikeda, M. Komura, H. Koike, K. Satoh, S. Itoh, Y. Shibata, Shallow sink in antenna pigment system of photosystem I of a marine centric diatom, *Chaetoceros gracilis* revealed by ultrafast fluorescence spectroscopy at 17 K, J. Phys. Chem. B 114 (2010) 9031–9038.
[22] A. Amunts, H. Toporik, A. Borovikova, N. Nelson, Structure determination and improved model of plant photosystem I, Nature 285 (2010) 3478–3486.
[23] S. Ozawa, T. Onishi, Y. Takahashi, Identification and characterization of an assembly intermediate subcomplex of photosystem I in the green alga *Chlamydomonas reinhardtii*, J. Biol. Chem. 285 (2010) 20072–20079.
[24] P. Jordan, P. Fromme, H.T. Witt, O. Klukas, W. Saenger, N. Krauss, Three-dimensional structure of cyanobacterial photosystem I at 2.5 Å resolution, Nature 411 (2001) 909–917.
[25] K. Satoh, A. Kamiesu, H. Egashira, Y. Yano, Y. Kashino, H. Koike, Crystallization of photosystem I complexes from the thermophilic cyanobacterium, *Synechococcus vulcanus*, Plant Cell Physiol. 40 (1999) 96–99.
[26] R. Bassi, D. Simpson, Chlorophyll–protein complexes of barley photosystem I, Eur. J. Biochem. 163 (1987) 221–230.
[27] R. Bassi, S.Y. Soen, G. Frank, H. Zuber, J.D. Rochaix, Characterization of chlorophyll a/b proteins of photosystem I from *Chlamydomonas reinhardtii*, J. Biol. Chem. 267 (1992) 25714–25721.
[28] Y. Kashino, H. Koike, K. Satoh, An improved sodium dodecyl sulfate–polyacrylamide gel electrophoresis system for the analysis of membrane protein complexes, Electrophoresis 22 (2001) 1004–1007.
[29] T. Masaki, M. Tanabe, K. Nakamura, M. Soejima, Studies on a new proteolytic enzyme from A chromobacter lyticus M497-1. I. Purification and some enzymatic properties, Biochim. Biophys. Acta 660 (1981) 44–50.
[30] C. Masutani, R. Kusumoto, A. Yamada, N. Dohmae, M. Yokoi, M. Yuasa, M. Araki, S. Iwai, K. Takio, F. Hanaoka, The XPV (xeroderma pigmentosum variant) gene encodes human DNA polymerase eta, Nature 399 (1999) 700–704.
[31] M. Yoshida, K. Higashi, L. Jin, Y. Machi, T. Suzuki, A. Masuda, N. Dohmae, A. Suganami, Y. Tamura, K. Nishimura, T. Toida, H. Tomitori, K. Kashiwagi, K. Igarashi, Identification of acrolein-conjugated protein in plasma of patients with brain infarction, Biochem. Biophys. Res. Commun. 391 (2010) 1234–1239.
[32] A. Zouni, J. Kern, J. Frank, T. Hellweg, J. Behlke, W. Saenger, K.D. Irrgang, Size determination of cyanobacterial and higher plant photosystem II by gel permeation chromatography, light scattering, and ultracentrifugation, Biochemistry 44 (2005) 4572–4581.
[33] M.A. Larkin, G. Blackshields, N.P. Brown, R. Chenna, P.A. McGettigan, H. McWilliam, F. Valentin, I.M. Wallace, A. Wilm, R. Lopez, J.D. Thompson, T.J. Gibson, D.G. Higgins, Clustal W and Clustal X version 2.0, Bioinformatics 23 (2007) 2947–2948.
[34] G. Perrière, M. Gouy, WWW-Query: an on-line retrieval system for biological sequence banks, Biochimie 78 (1996) 364–369.
[35] T. Hiyama, B. Ke, Difference spectra and extinction coefficients of P700, Biochim. Biophys. Acta 267 (1972) 160–171.
[36] K. Satoh, S. Katoh, A. Donner, W. Oettmeier, Binding affinities of oxidized and reduced forms of tetrahalogenated benzoquinones to the QB site in oxygen-evolving photosystem II particles from *Synechococcus elongatus*, Plant Cell Physiol. 35 (1994) 461–468.
[37] H. Koike, S. Katoh, Heat-stabilities of cytochromes and ferredoxin isolated from a thermophilic blue-green alga, Plant Cell Physiol. 20 (1979) 1157–1161.
[38] M. Komura, Y. Shibata, S. Itoh, A new fluorescence band F689 in photosystem II revealed by picosecond analysis at 4–77 K: function of two terminal energy sinks F689 and F695 in PS II, Biochim. Biophys. Acta 1757 (2006) 1657–1668.
[39] E.J. Stauber, A. Busch, B. Naumann, A. Svatoš, M. Hippler, Proteotypic profiling of LHCI from *Chlamydomonas reinhardtii* provides new insights into structure and function of the complex, Proteomics 9 (2009) 398–408.
[40] E.J. Stauber, A. Fink, C. Markert, O. Kruse, U. Johanningmeier, M. Hippler, Proteomics of *Chlamydomonas reinhardtii* light-harvesting proteins, Eukaryot. Cell 2 (2003) 978–994.
[41] J. Kargul, J. Nield, J. Barber, Three-dimensional reconstruction of a light-harvesting complex I-photosystem I (LHCI-PSI) supercomplex from the green alga *Chlamydomonas reinhardtii*, J. Biol. Chem. 278 (2003) 16135–16141.
[42] E. Wientjes, G.T. Oostergete, S. Jansson, E.J. Boekema, R. Croce, The role of Lhca complexes in the supramolecular organization of higher plant photosystem I, J. Biol. Chem. 284 (2009) 7803–7810.
[43] V.H. Schmid, S. Potthast, M. Wiener, V. Bergauer, H. Paulsen, S. Storf, Pigment binding of photosystem I light-harvesting proteins, J. Biol. Chem. 277 (2002) 37307–37314.
[44] J. Knoetzel, A. Mant, A. Haldrup, P.E. Jensen, H.V. Scheller, PSI-O, a new 10-kDa subunit of eukaryotic photosystem I, FEBS Lett. 510 (2002) 145–148.
[45] C. Vanselow, A.P.M. Weber, K. Krause, P. Fromme, Genetic analysis of the Photosystem I subunits from the red alga, *Galdieria sulphuraria*, Biochim. Biophys. Acta 1787 (2009) 46–59.
[46] Poul Erik Jensen, Anna Haldrup, Suping Zhang, H.V. Scheller, The PSI-O subunit of plant photosystem I is involved in balancing the excitation pressure between the two photosystems, J. Biol. Chem. 279 (2004) 24212–24217.
[47] J. Engelken, H. Brinkmann, I. Adamska, Taxonomic distribution and origins of the extended LHC (light-harvesting complex) antenna protein superfamily, BMC Evol. Biol. 10 (2010) 233.